Effect of Pt and Al content on the long-term, high temperature oxidation behavior and interdiffusion of a Pt-modified aluminide coating deposited on Ni-base superalloys

Nadia Vialas, Daniel Monceau *

CIRIMAT UMR 5085, ENSIACET-INPT, 31077 Toulouse Cedex 4, France

Abstract

The present work is devoted to the effect of Al and Pt content on the oxidation behavior and interdiffusion of the industrial NiPtAl coating RT22 deposited on SCB and IN792 Ni-base superalloys. Some specimens of RT22/SCB experienced a defective aluminization resulting in one side with a lower Al content, and some specimens of RT22/IN792 had less platinum than the specification. The effect of both Pt and Al on the initial microstructure of the coating is discussed. Isothermal oxidation tests for 100 h and long-term cyclic oxidation/interdiffusion tests at 1050 °C were performed (up to 51 cycles of 300 h). It is shown that a 50 μm coating with 30 at.% Al instead of a nominal 70 μm coating with 52 at.% Al leads to the full transformation of the β phase after 6 × 300 h at 1050 °C and to the formation of large voids and spinel oxides after 35 × 300 h, but also to less surface undulations than the standard coating. A lower Pt concentration in the RT22 coating results in lower aluminization kinetics and increased spalling and Al consumption during long-term cyclic oxidation without decreasing the isothermal oxidation kinetics.

Keywords: Diffusion; Phase transitions; Diffusion coatings; Nickel alloy

1. Introduction

Because of their good mechanical properties at high temperature, nickel-base superalloys are widely used for the hot components of aero engines, land based and marine gas turbines. To improve high temperature corrosion resistance, an alumina-forming protective coating is typically deposited on the superalloy [1]. Several studies have shown that platinum additions improve the performance of both alloy and aluminide coating [2–17]. Pt improves the oxide scale adherence [3,4,14,18–20], which is attributed to a reduction of growth stresses in the oxide scale [4], a mechanical keying by "pegs" formation [3] or an interaction with sulfur avoiding its detrimental effect [13,14,19,21]. Others studies showed that Pt reduces void formation at the metal/oxide interface [13,14,19,21–23]. This effect can be related to the effect of Pt on S segregation, since S is believed to promote interfacial void formation [24]. Another proposal is that Pt accelerates Al diffusion [25], then reduces the vacancies flux from the metal to the surface and inhibits vacancy coalescence and interfacial void formation. Some authors reported also that Pt has an effect on interdiffusion, slowing down the diffusive flux of alloying elements to the coating [6,8,11,13,26,27]. This effect on interdiffusion would reduce the formation of detrimental oxides [13]. It is also suggested that Pt promotes a selective alumina scale formation [6,7,11,23,28,29] and accelerates healing after spallation [13]. Pt accelerates slightly alumina scale growth and slows down transient alumina to α-alumina transformation [13,23,30,31]. Finally, Pt could have an effect on the stability of β-NiAl [13] and would delay its transformation to γ′-Ni_3Al [7]. But according to the Ni–Pt–Al phase diagram established by Gleeson and colleagues [32,33], Pt addition does not act significantly on the thermodynamic stability of β-NiAl when Al content decreases. The Al content in NiPtAl alloys determines the type of defects, activity and diffusion of elements. A lower Al content in β-NiAl

Table 1
Composition of SCB and IN792 superalloys

at.%	Ni	Cr	Co	Al	Ti	Ta	W	Mo	Hf	Zr	Fe
SCB	66	13	5	8.5	5.5	0.6	1.2	0.6			
IN792	60.1	13.5	9.0	7.6	5.0	1.3	1.2	1.2	0.2	0.1	0.5

* Corresponding author.
E-mail address: Daniel.Monceau@ensiacet.fr (D. Monceau).

doi:10.1016/j.surfcoat.2006.07.246

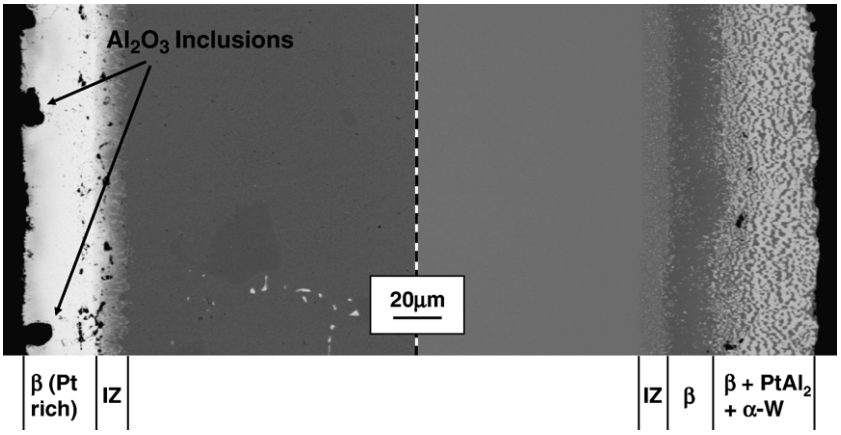

Fig. 1. Cross-section of the as-coated RT22/SCB: backscattered electron images of the low Al content side with inclusions of cement (left) and the well-aluminized side (right). IZ stands for Interdiffusion Zone.

decreases its resistance to cyclic oxidation [34]. Increasing the Al content of a Pt-modified beta aluminide coating has been shown to be beneficial [17].

In the present work, the industrial Pt-modified aluminide RT22 coating deposited on two Ni-base superalloys was studied. Fabrication of some specimens were inadvertently changed leading to samples with a lower Al content on one side and others with less Pt than the specification. Short-term isothermal and long-term cyclic oxidation tests were performed at 1050 °C. The effects of Al and Pt contents on initial and heat-treated microstructures and on oxidation kinetics are reported and discussed.

2. Experimental procedure

2.1. Materials

The test specimens (9 mm in diameter and 2 mm thick) were machined from single crystal nickel-base superalloy SCB or polycrystalline nickel-base superalloy IN792 (Table 1). They were coated with the industrial inward grown Pt-modified aluminide coating RT22. The process involves electrolytic deposition of 7±2 µm Pt, followed by heat treatment at 1010 °C under vaccum ($<10^{-3}$ Pa). Aluminization was then performed by pack cementation and the resulting coating homogenized at high temperature. Finally, the coated specimens were aged at a temperature depending on superalloy substrate [35]. On SCB, one side of the specimen was accidentally directly put on the cement resulting in a defective aluminization whereas the second side was correctly aluminized. On some IN792, the thickness of the electro-deposited Pt layer was below the specifications, leading to a coating with low Pt content.

2.2. Methods

Isothermal oxidation tests were performed on as-processed coated specimens in a Setaram TGA24S thermobalance for 100 h in synthetic flowing air at 1050 °C. Mass gain curves were

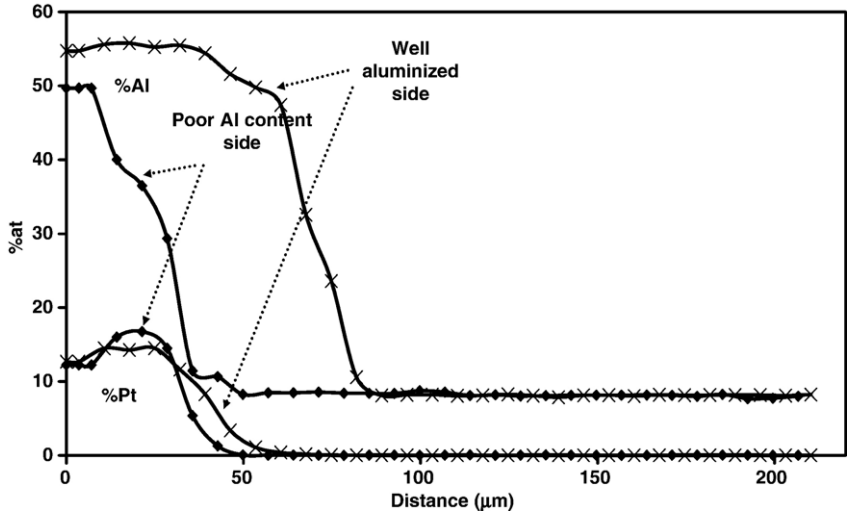

Fig. 2. Initial Al and Pt concentration profiles of the well-aluminized side and the low Al content side of RT22/SCB.

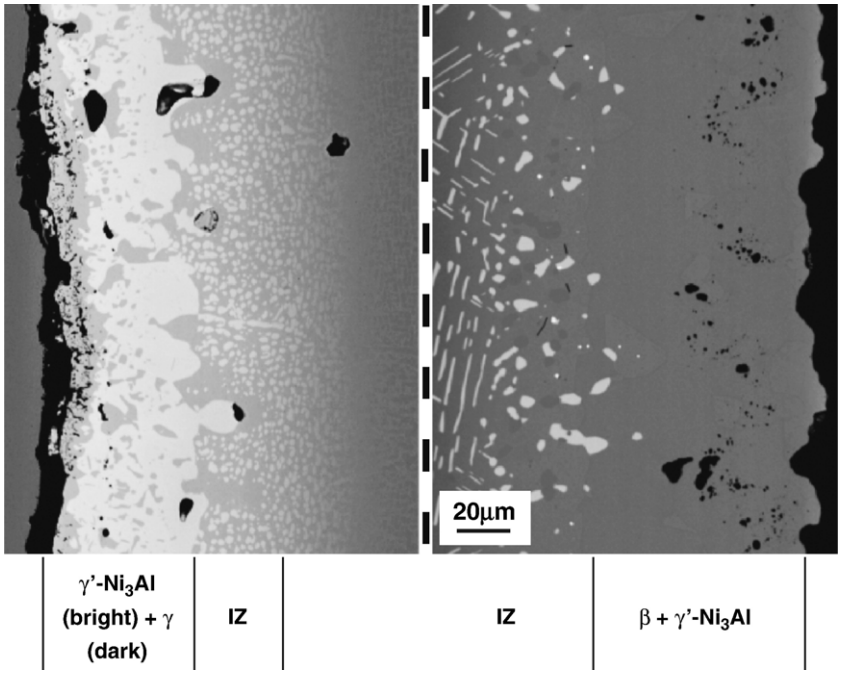

Fig. 3. Backscattered electron images of RT22/SCB after 6 cycles of 300 h at 1050 °C. Low Al content side (left) and well-aluminized side (right).

analyzed by local fitting to a general parabolic law [36]. Long-term and low frequency cycles (holding time of 300 h) were also performed at 1050 °C in still laboratory air as detailed in Ref. [35]. Before testing and after each cycle, specimens were weighted with an accuracy of 10 µg. Microstructural and chemical investigations were performed using a Leo 435 scanning electron microscope equipped with a PGT energy dispersive X-ray spectrometry system. The average concentration of elements was given by quantitative energy dispersive spectroscopy (EDS) analysis inside a 4 × 182 µm window translated from the metal/oxide interface to the substrate. Seiffert X-ray diffraction apparatus was used at 4° grazing incidence with $Cu_{k\alpha}$ radiation to identify the type of the oxides present in the oxide scales.

3. Experimental results

3.1. Effect of Al content

Fig. 1 compares the as-coated microstructure of the well-coated side and the low Al content side of the system RT22/SCB. The coating of the well-aluminized side is composed of a 40 µm external two-phase zone consisting of a mixture of β-NiAl and $PtAl_2$ phases and of bcc α-W precipitates. The 20 µm thick middle zone is a single-phase β-NiAl. The 10 µm thick interdiffusion zone contains three types of precipitates: bcc α-Cr, (Ti,Ta)-rich precipitates and tetragonal σ-phase. The total thickness of the coating is 70 µm. The quite different microstructure of the low Al content side consists of a 40 µm thick external layer composed of a Pt-rich β-NiAl phase with large alumina inclusions from the cement. The interdiffusion zone is 10 µm thick and composed of γ′-Ni_3Al. The total thickness of the coating is about 50 µm. Fig. 2 compares the concentration profiles of the standard and the low Al content sides. Concentration profile integration reveals that the average Al content within the low Al side coating is 30 at.% over 50 µm instead of 52 at.% over 70 µm for the standard side. This corresponds to an aluminum reservoir more than 2 times lower for the defective side. The two coatings have the same Pt content throughout.

As shown in Fig. 3, after 6 cycles of 300 h at 1050 °C, the oxide scale formed on the correctly aluminized side is undulated whereas the oxide scale grown on the low Al content side is smoother. In the low Al content side, the coating is mainly composed of a bright γ′-Ni_3Al phase with an Al content of 13 at.% and a darker γ phase with 5 at.% Al. Some voids are observed close to the metal/oxide interface but also deeper in the substrate. The presence of such deep voids in the low Al content side is confirmed by the cross-sectional images of RT22/SCB after 35 cycles of 300 h (Fig. 4).

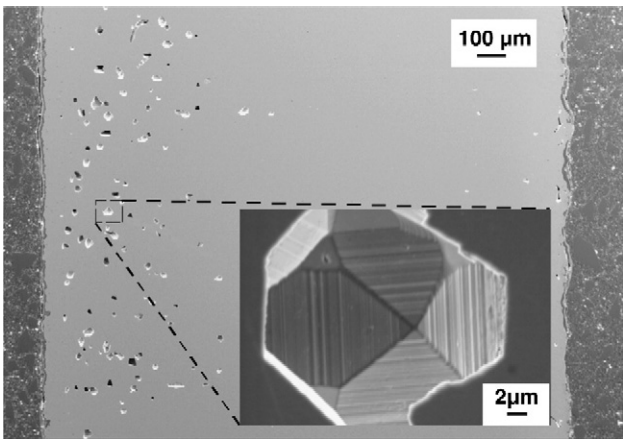

Fig. 4. Cross-section of RT22/SCB after 35 cycles of 300 h at 1050 °C, low Al content side on the left with large Kirkendall voids. Enlargement of one void.

3.2. Effect of Pt content

As-coated microstructure of the system RT22/IN792 with a standard Pt content is compared to the same system with a low Pt content in Fig. 5. Low Pt level results in a thinner coating (62 μm instead of 80 μm) and is composed of a 15 μm external zone containing β-NiAl enriched in Pt, a 25 μm middle zone containing β-NiAl and a 22 μm interdiffusion zone. Types of precipitates are the same irrespective of the thickness of the initial Pt deposit. The average composition of the coating was calculated integrating atomic concentration profiles from the surface to the interdiffusion zone/substrate interface. The coating with less Pt (0.7 at.% instead of 5.4 at.%) also contains less Al (35 at.% instead of 43 at.%).

Thermogravimetry analysis was performed on coatings with standard and low Pt contents. The mass gains follow parabolic kinetics after a transient stage of faster kinetics (Fig. 6). The instantaneous parabolic rate constant, k_p, was calculated as a function of time and its evolution for the first 2 h is also shown in Fig. 6. The low Pt coating had an oxide scale growth rate slightly lower than the regular coating with a shorter transient regime.

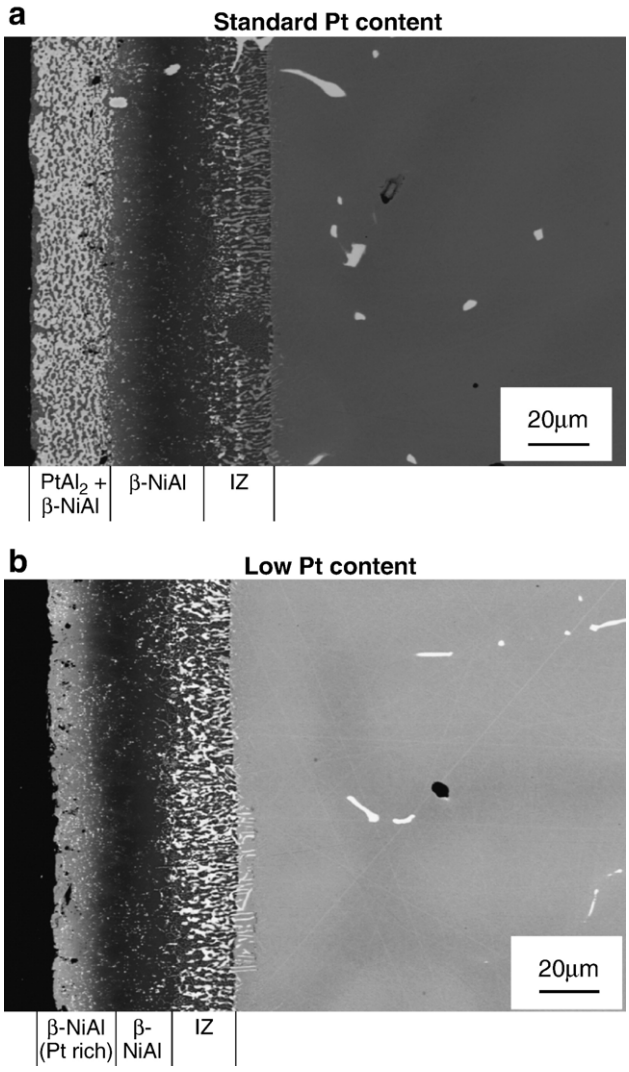

Fig. 5. Backscattered electron images of as-coated RT22/IN792 with standard Pt content (a) and with low Pt content (b).

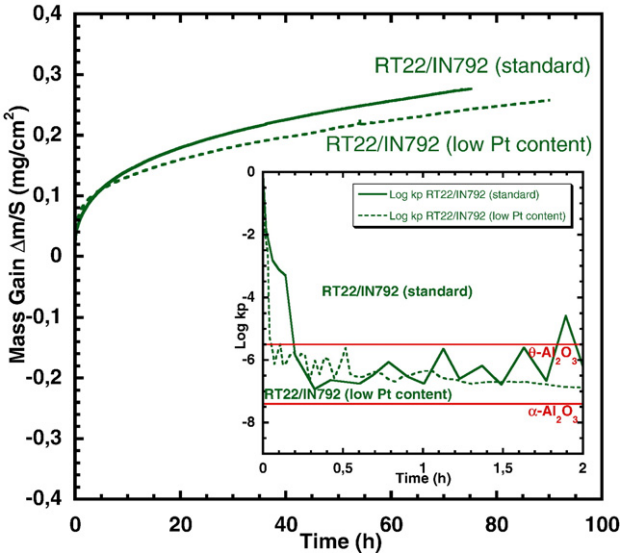

Fig. 6. Mass gain curves and k_p evolution during transient stage at 1050 °C of RT22/IN792 with standard and with low Pt contents.

Long-term cyclic oxidation kinetics of RT22/IN792 specimens with low and standard Pt content are given in Fig. 7. These results show the better cyclic oxidation resistance of the standard Pt level samples. This observation, combined with the isothermal thermogravimetry results, shows that the beneficial effect of Pt on cyclic oxidation resistance is due to a decrease of oxide scale spalling and not to lower isothermal oxidation kinetics (Fig. 6). After 100 h at 1050 °C, the coating with a low Pt concentration experiences spalling whereas no spalling is observed for the standard coating. However, XRD indicates that the type of oxides formed is the same whatever the Pt content, except for γ-Al_2O_3 which is detected only on RT22/IN792 with a standard Pt content [30]. This observation indicates that Pt delayed the transformation of transient alumina to α-alumina, as suggested by thermogravimetry analysis. Moreover, SEM observation [30] reveals short whiskers which are a typical morphology for the metastable alumina in which growth by cation diffusion predominates [37]. SEM images of surfaces after 6 cycles and 17 cycles in BSE mode allowing an easier quantification of oxide scale spalling [38], show that spalling increases with lower Pt content. After 6 and 8 cycles of 300 h, XRD analysis showed that spinels formed on RT22/IN792 with low Pt content whereas after 7 and 17 cycles of 300 h, no spinel formed on RT22/IN792 with standard Pt content [30].

Consumption of Al by oxidation, spallation and diffusion and the interdiffusion of alloying elements lead to microstructural changes. According to the Ni–Pt–Al phase diagram [33], the sequence of phase transformations within the coating is β-NiAl → γ′-Ni_3Al → γ. Backscattered electron images of the low and standard Pt content specimens after 6 × 300 h at 1050 °C are shown in Fig. 8. The coating with a standard Pt content is still mainly composed of β with some γ′ grains in the

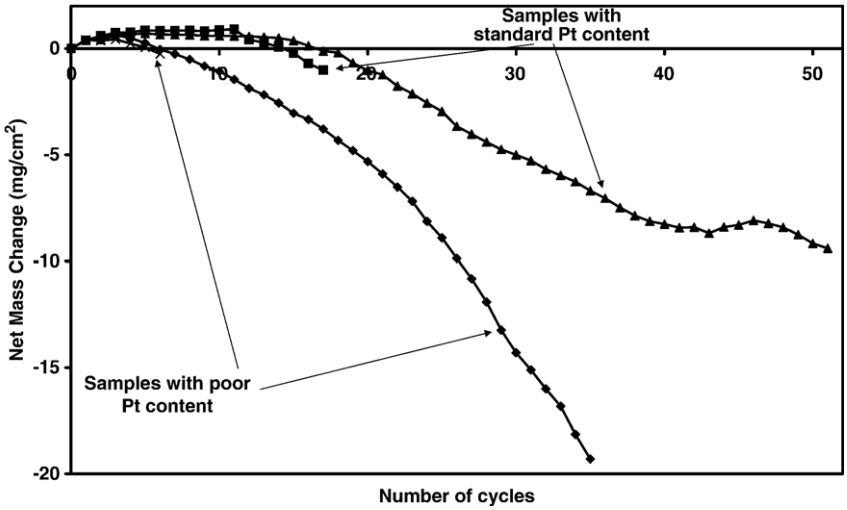

Fig. 7. Net mass change (NMC) curves at 1050 °C of RT22/IN792 specimens with a standard Pt content and with a low Pt content.

middle zone. After the same treatment, the low Pt coating developed a 10 μm single-phase γ′ zone parallel to the metal/oxide interface. The middle zone of the coating is a mixture of β and γ′. Between this two-phase layer and the interdiffusion zone, a γ′ single-phase zone is observed due to interdiffusion between the coating and the substrate. This microstructure after 6×300 h is quite similar to the microstructure of the coating with a standard Pt content after 17 cycles of 300 h [30].

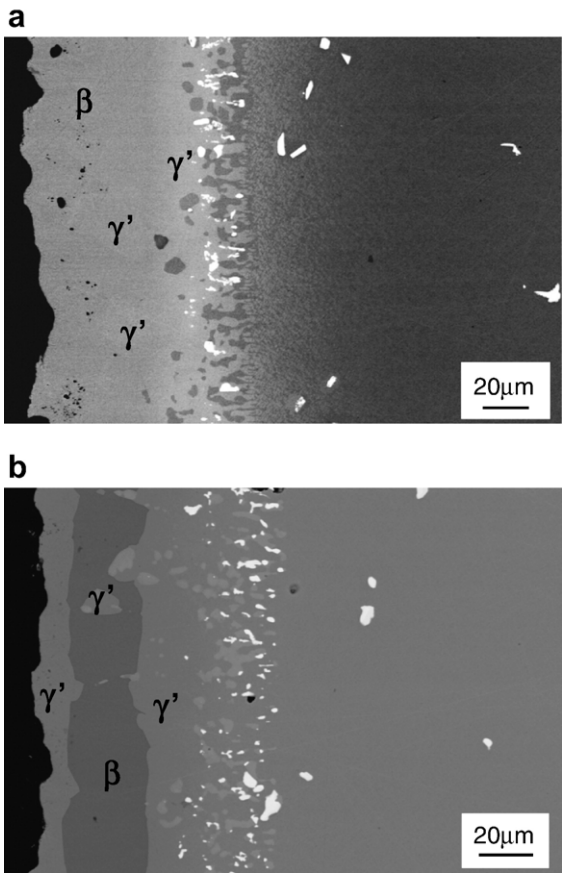

Fig. 8. Microstructural evolution of RT22/IN792 with standard Pt content (a) and low Pt content (b) after 6 cycles of 300 h at 1050 °C.

4. Discussion

4.1. Voids formation in the low Al content side

In the specimen with a defective aluminization, many voids are formed in the low Al content side (Fig. 4). The formation of such voids can be explained by a flux of vacancies from the surface toward the superalloy. During high temperature treatment, two Al fluxes occur. The first one, from the coating toward the surface, is due to the Al consumption to form the protective oxide scale. The second one, from the coating toward the superalloy substrate is due to interdiffusion. In the same way, a Pt flux from the coating to the superalloy and fluxes of Ni and others alloying elements exist. In the low Al content side, the initial Al reservoir is quickly consumed and the coating then becomes poorer in Al than the superalloy after 10,500 h. Following a Kirkendall mechanism, vacancies are created at vacancy sources in the coating and diffuse towards the superalloy. The vacancies coalesce to form voids in the superalloy at vacancy sinks.

4.2. Surface undulations

During long-term low frequency cyclic oxidation, undulations develop at the coating surface. This is a well-known problem for β aluminide coatings and several explanations have been proposed and recently reviewed in Refs. [39,40]. We observed in the present work that these undulations are larger on the well-aluminized side. As the cycle frequency is very low (300 h cycles), the martensitic transformation in the beta phase [39] or the reversible high temperature γ′ to β [40] unlikely cause these undulations. Two mechanisms may explain this undulated morphology. The first is that the low Al side of the sample has a lower initial β phase content and then experiences less volume reduction during its transformation to γ′. The

alternative explanation is that the undulations result from the movement of the oxide/coating interface: on the defective side of the sample, there is less surface recession because vacancies are not annihilated at the interface but coalesce inside the metal to form voids.

4.3. Effect of Pt content

In this study, the behavior of two samples fabricated with two initial Pt layer thicknesses are compared. The first improvement induced by the higher Pt level is to increase the amount of Al introduced during the aluminizing process, confirming the results of Benoist et al. [41]. The present work also shows that Pt increases slightly the isothermal oxide scale growth rate and slows down the transformation of the transient to alpha alumina. The slowing down of this reaction with its associated oxide volume reduction could allow some relaxation of growth stresses, improving the oxide scale adherence. Cyclic oxidation tests show clearly that Pt improves adherence of the oxide scale. Then, aluminum consumption by successive oxidation/spallation is slower in the coating with standard Pt content and consequently the transformation of β-NiAl to γ′-Ni_3Al and to γ-Ni is delayed as well as the formation of oxides having a fast growth rate such as spinels.

5. Conclusion

This paper demonstrates that a good quality fabrication of the coating is essential for its resistance against long-term high temperature cyclic oxidation. A lower Al level after aluminization induces the formation of large voids. Nevertheless, the coating with the higher Al content experiences more interfacial undulations despite the low thermal cycling frequency. The deposit of a Pt layer with its thickness under specification is also detrimental because of the associated decrease of the oxide scale adherence and because of an induced lower initial level of Al. The overall consequence of these effects is a lower resistance to cyclic oxidation for the nickel aluminide coating containing 0.7 at.% Pt in comparison with the standard coating with 5.4 at. % Pt.

Acknowledgments

The authors thank EEC for the financial support through the European project Allbatros N°ENK5-CT2000-00081 and all partners for their contribution. Sincere thanks are expressed to Prof. B. Pieraggi for the fruitful discussions and the helpful comments on the manuscript.

References

[1] J.R. Nicholls, MRS Bull. (Sept (2003)) 659.
[2] G. Lehnert, H.W. Meinhardt, Electrodepos. Surf. Treat. 1 (1972) 189.
[3] E.J. Felten, F.S. Pettit, Oxid. Met. 10 (1976) 189.
[4] J.G. Fountain, F.A. Golightly, F.H. Stott, G.C. Wood, Oxid. Met. 10 (1976) 341.
[5] F.A. Golightly, F.H. Stott, G.C. Wood, Oxid. Met. 10 (1976) 163.
[6] G.H. Meier, F.S. Pettit, Surf. Coat. Technol. 39/40 (1989) 1.
[7] Y. Niu, W.T. Wu, D.H. Boone, J.S. Smith, J.Q. Zhang, C.L. Zhen, J. Phys. 3 (1993) 511.
[8] H.M. Tawancy, N.M. Abbas, T.N. Rhys-Jones, Surf. Coat. Technol. 49 (1991) 1.
[9] H.M. Tawancy, N.M. Abbas, T.N. Rhys-Jones, Surf. Coat. Technol. 54–55 (1992) 1.
[10] H.M. Tawancy, N. Sridhar, B.S. Tawabini, N.M. Abbas, T.N. Rhys-Jones, J. Mater. Sci. 27 (1992) 6463.
[11] H.M. Tawancy, N. Sridhar, N.M. Abbas, D. Rickerby, Scr. Mat. 33 (1995) 1431.
[12] G.R. Krishna, D.K. Das, V. Singh, S.V. Joshi, MSE A 251 (1998) 40.
[13] J.A. Haynes, Y. Zhang, W.Y. Lee, B.A. Pint, I.G. Wright, K.M. Cooley, Elevated Temp. Coat.: Sci. Technol. III (1999) 185.
[14] Y. Zhang, W.Y. Lee, J.A. Haynes, I.G. Wright, B.A. Pint, K.M. Cooley, P.K. Liaw, Metall. Mater. Trans. 30A (1999) 2679.
[15] C. Leyens, B.A. Pint, I.G. Wright, Surf. Coat. Technol. 133–134 (2000) 15.
[16] B.A. Pint, J.A. Haynes, K.L. More, I.G. Wright, C. Leyens, Superalloys 2000, TMS, 2000, 629–638.
[17] D.K. Das, V. Singh, S.V. Joshi, Oxid. Met. 57 (2002) 245.
[18] J.A. Haynes, M.K. Ferber, W.D. Porter, E.D. Rigney, Oxid. Met. 52 (1999) 31.
[19] Y. Zhang, J.A. Haynes, W.Y. Lee, I.G. Wright, B.A. Pint, K.M. Cooley, P.K. Liaw, Metall. Mater. Trans. 32A (2001) 1727.
[20] J.H.W. deWit, P.A. van Manen, Mat. Sci. Forum 154 (1994) 109.
[21] J.A. Haynes, B.A. Pint, K.L. More, Y. Zhang, I.G. Wright, Oxid. Met. 58 (2002) 513.
[22] Y. Cadoret, M.-P. Bacos, P. Josso, V. Maurice, P. Marcus, S. Zanna, Mat. Sci. Forum (2004) 247.
[23] I. Wright, B. Pint, R. Judkins, First International Conference on Industrial Gas Turbine Technologies, Brussels, 2003.
[24] H.J. Grabke, D. Wiemer, H. Viefhaus, Appl. Surf. Sci. 47 (1991) 243.
[25] R. Bouchet, R. Mevrel, Calphad 27 (2003) 295.
[26] M.R. Jackson, J.R. Rairden, Metall. Mater. Trans. 8A (1977) 1697.
[27] A.L. Purvis, B.M. Warnes, Surf. Coat. Technol. 146–147 (2001) 1.
[28] Angenete, J., PhD thesis, Chalmers University of Technology, 2002.
[29] D.K. Das, M. Roy, V. Singh, S.V. Joshi, Mater. Sci. Technol. 15 (1999) 1199.
[30] Vialas, N., PhD thesis, INPT, 2004.
[31] Y. Cadoret, D. Monceau, M.-P. Bacos, P. Josso, V. Maurice, P. Marcus, Oxid. Met. 64 (2005) 185.
[32] B. Gleeson, W. Wang, S. Hayashi, D. Sordelet, Mat. Sci. Forum (2004) 213.
[33] S. Hayashi, S.I. Ford, D.J. Young, D.J. Sordelet, M.F. Besser, B. Gleeson, Acta Mater. 53 (2005) 3319.
[34] M.P. Brady, B.A. Pint, P.F. Tortorelli, I.G. Wright, R.J. Hanrahan, Materials Science and Technology, 2000, p. 230, Chapter 6.
[35] N. Vialas, D. Monceau, Oxid. Met. in press.
[36] D. Monceau, B. Pieraggi, Oxid. Met. 50 (1998) 477.
[37] J. Doychak, J.L. Smialek, T.E. Mitchell, Metall. Mater. Trans. A20 (1989) 499.
[38] N. Vialas, D. Monceau, B. Pieraggi, Mat. Sci. Forum 461–464 (2004) 747.
[39] A.W. Davis, A.G. Evans, Acta Mater. 53 (7) (2005) 1895.
[40] B.A. Pint, S.A. Speakman, C.J. Rawn, Y. Zhang, JOM 1 (2006) 47.
[41] J. Benoist, K.F. Badawi, A. Malié, C. Ramade, Surf. Coat. Technol. 182 (2003) 14.